

# Spectra and elliptic flow of (multi-)strange hadrons at RHIC and LHC within viscous hydrodynamics+hadron cascade hybrid model

Xiangrong Zhu\*

*School of Science, Huzhou University, Huzhou 313000, P.R. China and  
Department of Physics and State Key Laboratory of Nuclear Physics and Technology,  
Peking University, Beijing 100871, P.R. China*

Using the (2+1)-dimensional ultrarelativistic viscous hydrodynamics+hadron cascade, VISHNU, hybrid model, we study the  $p_T$ -spectra and elliptic flow of  $\Lambda$ ,  $\Xi$ , and  $\Omega$  in Au+Au collisions at  $\sqrt{s_{NN}}=200$  GeV and in Pb+Pb collisions at  $\sqrt{s_{NN}}=2.76$  TeV. Comparing our model results with the data measurements, we find that the VISHNU model gives good descriptions of the measurements of these strange and multi-strange hadrons at several centrality classes at RHIC and LHC. Mass ordering of elliptic flow  $v_2$  among  $\pi$ ,  $K$ ,  $p$ ,  $\Lambda$ ,  $\Xi$ , and  $\Omega$  are further investigated and discussed at the two collision systems. We find, at both RHIC and LHC, the  $v_2$  mass ordering among  $\pi$ ,  $K$ ,  $p$ , and  $\Omega$  are fairly reproduced within the VISHNU hybrid model, and more improvements are needed to implement for well describing the  $v_2$  mass ordering among  $p$ ,  $\Lambda$ , and  $\Xi$ .

PACS numbers: 12.38.Mh, 5.75.Gz, 25.75.Ld, 24.10.Nz

## I. INTRODUCTION

Ultrarelativistic heavy-ion collisions at the BNL Relativistic Heavy Ion Collider (RHIC) and CERN Large Hadron Collider (LHC) are used to produce and study a hot and dense medium consisting of strongly interacting quarks and gluons, namely Quark-Gluon Plasma (QGP), which is expected to exist in the early stage of the universe, and to understand its properties, such as the equation of state (EoS), transport coefficients. The hadronic interactions are expected to have less influence on the multi-strange hadrons, such as  $\Xi$  and  $\Omega$ , due to their much smaller hadronic cross sections. Therefore, final observables of these multi-strange hadrons are more sensitive to the early (partonic) stage of the collision. In the past few decades, different aspects of strange and multi-strange hadrons have been investigated theoretically [1–13] and experimentally [14–24].

Anisotropic flow, which is considered as an evidence for the QGP formation, typically displays the collective behavior of the final emitted particles. It can be characterized by the coefficients of the Fourier expansion of the final particle azimuthal distribution defined as [25]:

$$E \frac{d^3 N}{d^3 p} = \frac{1}{2\pi} \frac{d^2 N}{p_T dp_T dy} \left( 1 + 2 \sum_{n=1}^{\infty} v_n \cos[n(\varphi - \Psi_n)] \right) \quad (1)$$

where  $v_n$  is the  $n^{\text{th}}$  order anisotropic flow harmonic with its corresponding reaction plane angle  $\Psi_n$ , and  $\varphi$  is the azimuthal angle of the final emitted particles. Recently, the anisotropic flow and other soft hadron data of all charged and identified hadrons at the RHIC and LHC have been studied by many groups within the framework of hydrodynamics [13, 26–36]. VISHNU is a hybrid

model [37] for single-shot simulations of heavy-ion collisions, which connects the (2+1)-dimensional viscous hydrodynamics with a hadronic afterburner. Employing the VISHNU hybrid model, the specific QGP shear viscosity value of  $(\eta/s)_{QGP}$  are extracted from the elliptic flow measurements of charged hadrons with MC-KLN initial conditions [29]. With the extracted  $(\eta/s)_{QGP}$ , the VISHNU provides good descriptions of the soft hadron data of  $\pi$ ,  $K$ , and  $p$  at the RHIC and LHC [30]. Compared with other hadrons, anisotropy flow of (multi-)strange particles are mainly produced in the QGP stage and less contaminated by the subsequent hadronic interactions. Meanwhile, the  $p_T$ -spectra and elliptic flow for  $\Lambda$ ,  $\Xi$ , and  $\Omega$  have been measured in the Au+Au collisions at the RHIC [17–20] and Pb+Pb collisions at the LHC [21–23]. Therefore, it is timely to systematically study these strange and multi-strange hadrons at RHIC and LHC via the VISHNU hybrid model.

In this paper, we investigate the  $p_T$ -spectra and elliptic flow  $v_2$  for (multi-)strange hadrons in Au+Au collisions at  $\sqrt{s_{NN}}=200$  GeV and in Pb+Pb collisions at  $\sqrt{s_{NN}}=2.76$  TeV within the viscous hydrodynamic hybrid model VISHNU. The paper is organized as follows. Section II briefly introduces the VISHNU hybrid model and its setup in the calculations. Section III compares our VISHNU results in Au+Au collisions and Pb+Pb collisions with the measurements from the STAR at RHIC and ALICE at LHC, respectively, mainly including  $p_T$ -spectra and differential elliptic flow for  $\Lambda$ ,  $\Xi$ , and  $\Omega$ . In Sec. IV, the mass ordering of elliptic flow among  $\pi$ ,  $K$ ,  $p$ ,  $\Lambda$ ,  $\Xi$ , and  $\Omega$  is studied and discussed at the RHIC and LHC energies. Finally, we summarize our works and give a brief outlook for the future in Sec. V.

## II. SETUP OF THE CALCULATION

We here give brief descriptions of the inputs and setup of VISHNU calculations for the soft data at the RHIC and

\* Correspond to [xrongzhu@pku.edu.cn](mailto:xrongzhu@pku.edu.cn); [xrongzhu@zjhu.edu.cn](mailto:xrongzhu@zjhu.edu.cn)

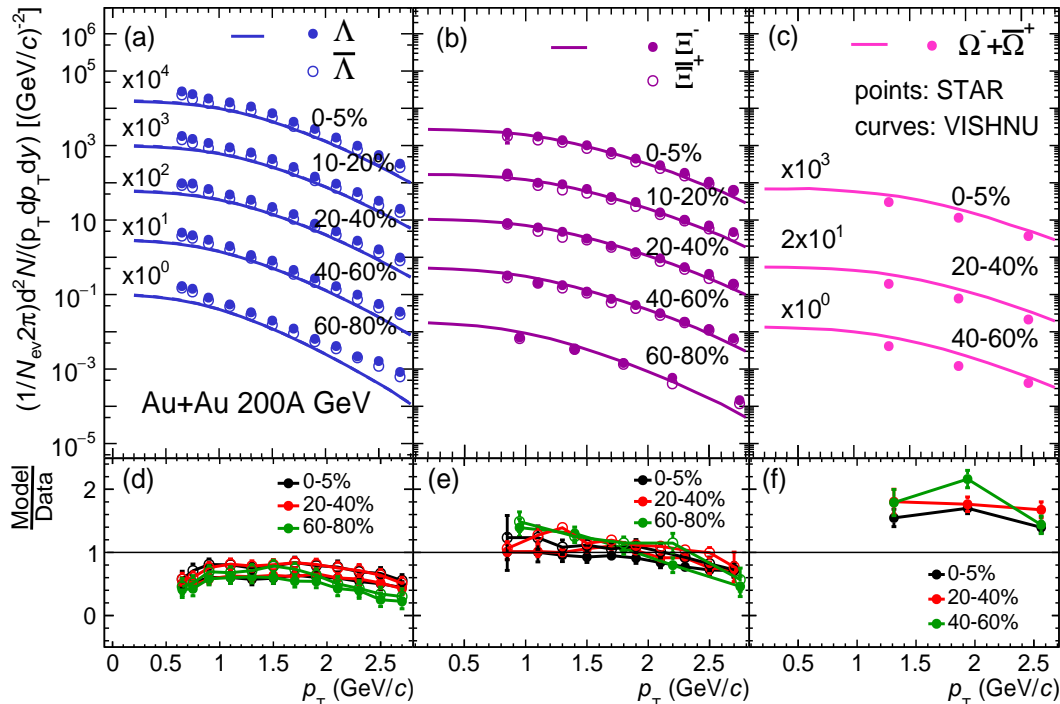


FIG. 1. (Color online) Transverse momentum spectra of  $\Lambda$  ( $\bar{\Lambda}$ ),  $\Xi^-$  ( $\bar{\Xi}^+$ ) and  $\Omega^- + \bar{\Omega}^+$  at various centralities in Au+Au collisions at  $\sqrt{s_{NN}}=200$  GeV. Experimental data are taken from STAR measurements [15]. Theoretical curves are calculated by the VISHNU hybrid model with the parameters presented in Sec. II. From top to bottom the curves correspond to 0-5% ( $\times 10^4$ ), 10-20% ( $\times 10^3$ ), 20-40% ( $\times 10^2$ ), 40-60% ( $\times 10^1$ ), and 60-80% ( $\times 10^0$ ) centrality, respectively, where the factors in parentheses are the multipliers applied to the spectra for clear separation. The multiplied factor for spectra of  $\Omega$  at 20-40% is  $2 \times 10^1$  instead of  $1 \times 10^1$ . In VISHNU, the spectra of particles and corresponding anti-particles are same due to zero net-baryon density used in our calculations. Therefore, only results of particles are shown with solid curves.

LHC energies. The VISHNU [37] hybrid model consists of two parts, which are the (2+1)-dimensional ultrarelativistic viscous hydrodynamics VISH2+1 [38, 39] for the expansion of strongly interacting matter QGP and a microscopic hadronic cascade model (UrQMD) [40, 41] for the hadronic evolution. In the calculations a switching temperature  $T_{sw}$  of 165 MeV is set for the transition from the macroscopic to microscopic approaches in VISHNU. This switching temperature value is close to the QCD phase transition temperature [42–45]. We input the equation of state (EOS) s95p-PCE [46, 47] for the hydrodynamic evolution above the switching temperature  $T_{sw}$ . The s95p-PCE, which accounts for the chemical freeze-out at  $T_{chem}=165$  MeV, was constructed by combing the lattice QCD data at high temperature with a chemically frozen hadron resonance gas at low temperature.

Following Refs. [29, 30], we input MC-KLN initial conditions [48–50] and start the hydrodynamic simulations at  $\tau_0 = 0.9$  fm/c. For improving computational efficiency, we implement single-shot simulations [13, 29, 30, 37, 51, 52] with smooth initial entropy density profiles generated by the MC-KLN model. The smooth initial entropy densities are obtained by averaging over a large number of fluctuating entropy density profiles within a specific centrality class. The initial density profiles are initial-

ized with the reaction plane method, which was once used in [29, 30, 52]. Considering the conversion from total initial entropies to final multiplicity of all charged hadrons, we do the centrality selection through the distribution of total initial entropies that are obtained from the event-by-event fluctuating profiles. Such centrality classification was firstly used by Shen in Ref. [53], which is more close to the experimental one defined from the measured multiplicity distributions. The normalization factors for the initial entropy densities in Au+Au collisions and Pb+Pb collisions are respectively fixed to reproduce the charged hadron multiplicity density  $dN_{ch}/d\eta$  with  $687.4 \pm 36.6$  at the RHIC [54] and  $1601 \pm 60$  at the LHC [55] at most central collisions. The  $\lambda$  parameter in the MC-KLN model, which quantifies the gluon saturation scale in the initial gluon distributions [49], is tuned to 0.218 at the RHIC and 0.138 at the LHC for a better description of the centrality dependent multiplicity density for all charged hadrons.

In the VISHNU simulations with MC-KLN initial conditions, we set a value of 0.16 for the QGP specific shear viscosity  $(\eta/s)_{QGP}$ . Such combined setting in VISHNU calculations once nicely described the elliptic flow of  $\pi$ ,  $K$ , and  $p$  in Au+Au collisions [51] and Pb+Pb collisions [30]. Here, we continue to use it to further study the

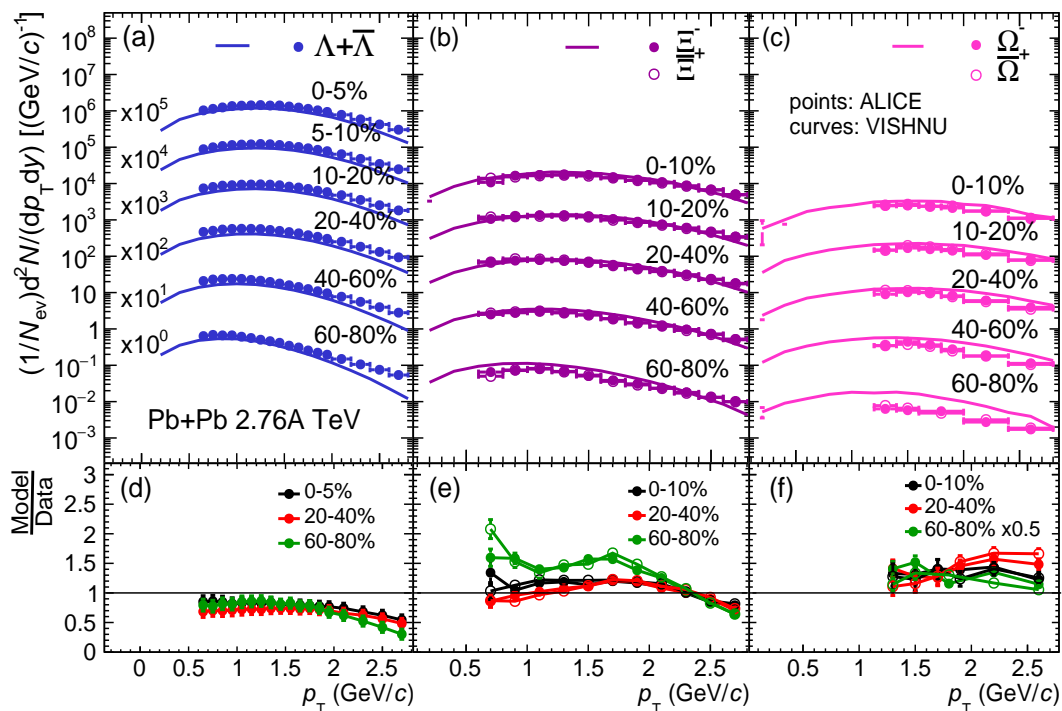


FIG. 2. (Color online) Transverse momentum spectra of  $\Lambda + \bar{\Lambda}$ ,  $\Xi^- (\bar{\Xi}^+)$  and  $\Omega^- (\bar{\Omega}^+)$  at various centralities in Pb+Pb collisions at  $\sqrt{s_{NN}} = 2.76$  TeV. Experimental data are taken from LHC [21, 22]. Theoretical curves are calculated with the VISHNU hybrid model with the parameters presented in Sec. II. From top to bottom the curves correspond to 0-10% ( $\times 10^4$ ), 10-20% ( $\times 10^3$ ), 20-40% ( $\times 10^2$ ) and 60-80% ( $\times 10^0$ ) centrality, respectively, where the factors in parentheses are the multipliers applied to the spectra for clear separation. Spectra of  $\Lambda$  start from 0-5% ( $\times 10^5$ ) and 5-10% ( $\times 10^4$ ), instead of 0-10%. In VISHNU, the spectra of particles and corresponding anti-particles are same due to zero net-baryon density used in our calculations. Therefore, only results of particles are shown with solid curves.

soft hadron data of strange and multi-strange hadrons at both RHIC and LHC. For simplicity the theoretical calculations, we neglect the bulk viscosity, net baryon density, and the heat conductivity in the QGP system evolution.

### III. SPECTRA AND ELLIPTIC FLOW

In Fig. 1, we present the transverse momentum spectra of hadrons  $\Lambda$ ,  $\Xi$ , and  $\Omega$  in Au+Au collisions at  $\sqrt{s_{NN}} = 200$  GeV from the VISHNU hybrid model, and compare these results with the STAR measurements. We observe that the VISHNU generally describes the  $p_T$ -spectra  $\Xi$ , but slightly overestimates the production of  $\Omega$  at all centrality classes. Our VISHNU results of  $\Lambda$  at  $p_T < 2$  GeV/c are about 40% lower than  $\Lambda$  from STAR, and about 20% lower than  $\bar{\Lambda}$  from STAR. This can be understood from following. In our calculations, the production of  $\Lambda$  is obtained from the original values of strong resonance decays from UrQMD of VISHNU. For the STAR measurements, the  $\Lambda$  spectra are corrected for the feed-down of multi-strange baryon weak decays (the feed-down contributions to the  $\Xi$  spectra from  $\Omega$  decays are negligible) [15]. Meanwhile, the STAR  $\Lambda$  spectra are

not subtracted the contribution from  $\Sigma^0$  from the channel of  $\Sigma^0 \rightarrow \Lambda + \gamma$ <sup>1</sup>. At LHC, it was found that the contribution from  $\Sigma^0$  for  $\Lambda$  is about 30% in VISHNU calculations [52]. Furthermore, we notice that STAR measurements of  $\Lambda$  and  $\Xi^-$  are slightly larger than their corresponding anti-particles due to non-zero baryon density at this collision energy. In our calculations, however, zero net baryon density is used, which leads to the same results between these (multi)-strange hadrons and their anti-particle partners.

We also calculate the transverse momentum spectra of  $\Lambda$ ,  $\Xi$ , and  $\Omega$  in Pb+Pb collisions at LHC with our VISHNU hybrid model. The calculations, compared with the measurements from the ALICE Collaboration, are presented in Fig. 2. For the ALICE measurements, the production differences between these (multi)-strange hadrons and their anti-particles are very small due to very small net baryon density at the LHC energies. It also shows that the VISHNU generally describes the  $p_T$ -spectra of hadrons  $\Lambda$ ,  $\Xi$ , and  $\Omega$  at several centrality classes, except for the 60-80% centrality bin. Here, our theoretical calculations of  $\Lambda$  only include strong resonance decays from UrQMD of

<sup>1</sup> For  $\bar{\Lambda}$ , the contribution from  $\bar{\Sigma}^0$  is via the channel of  $\bar{\Sigma}^0 \rightarrow \bar{\Lambda} + \gamma$ .

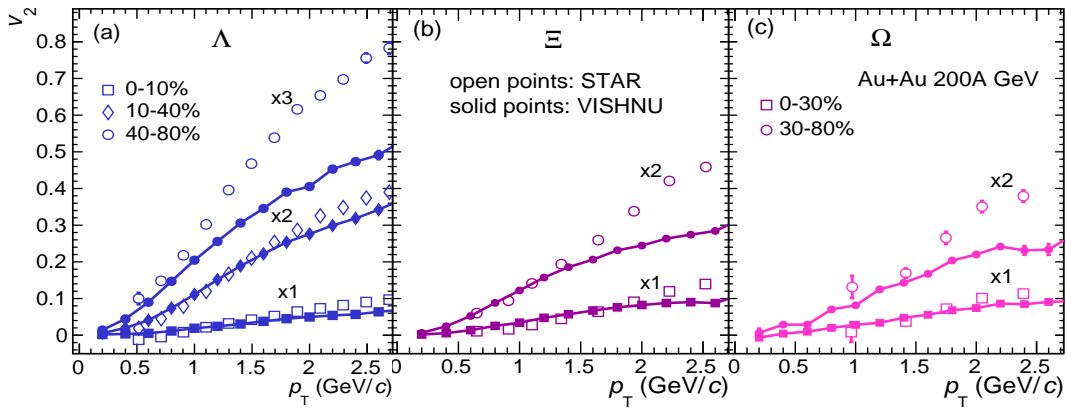


FIG. 3. (Color online) Differential elliptic flow of strange hadrons  $\Lambda$  (left) at centralities of 0-10% (squares), 10-40% (diamonds), and 40-80% (circles), and multi-strange hadrons  $\Xi$  (middle) and  $\Omega$  (right) at centralities of 0-30% (squares), 30-80% (circles) in Au+Au collisions at  $\sqrt{s_{NN}}=200$  GeV. Experimental data (open points) are from STAR [19, 20]. Theoretical results (solid points) are calculated from the VISHNU viscous hydrodynamics hybrid model with the inputs presented in Sec. II.

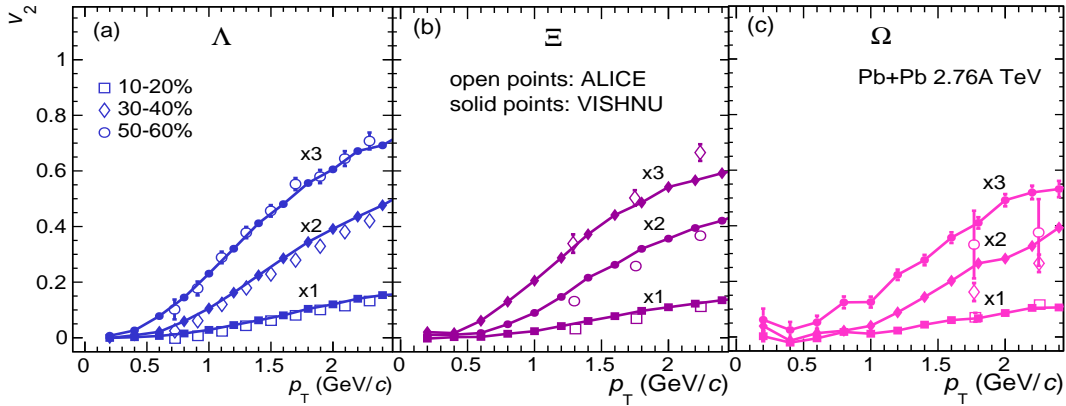


FIG. 4. (Color online) Differential elliptic flow of strange hadrons  $\Lambda$  (left), multi-strange hadrons  $\Xi$  (middle) and  $\Omega$  (right) at 10-20% (squares), 30-40% (diamonds), and 50-60% (circles) centralities in Pb+Pb collisions at  $\sqrt{s_{NN}}=2.76$  TeV. Experimental data (open points) are from the ALICE measurements [23]. Theoretical results (solid points) are calculated from the VISHNU hybrid model with the inputs presented in Sec. II, which were first shown in Ref. [52].

VISHNU. As a result, they are about 30% lower than the ALICE measurements including contribution from non-weak decays of  $\Sigma^0$  and  $\Sigma(1385)$  family [21]. The  $\Omega$  spectra from VISHNU are slightly higher than the experimental data at these centrality classes, as similarly observed in the calculations at the RHIC. Such deviations between theory and experiment are consistent with the model and data differences for the centrality dependent multiplicity shown in [52].

From comparisons between our calculations and measurements at the RHIC and LHC, we find that, although the VISHNU can not fully reproduce the  $p_T$ -spectra of these strange and multi-strange hadrons in the production amount, it gives nice descriptions of the slopes (distribution shapes) for the spectra of them at various centralities. This can be found from the ratio between model results and data in Fig. 1 and 2, which are weakly centrality dependent. Together with the early nice descriptions

of the  $p_T$ -spectra for  $\pi$ ,  $K$ , and  $p$  [30], it reveals that during the QGP and hadronic evolution the VISHNU hybrid model generates a proper amount of radial flow to push the spectra of various hadrons.

Figure 3 presents the comparisons of differential elliptic flow of  $\Lambda$ ,  $\Xi$ , and  $\Omega$  from the VISHNU model with the STAR measurements in Au+Au collisions at  $\sqrt{s_{NN}}=200$  GeV. The theoretical curves are calculated from VISHNU model by using reaction plane initial conditions from the MC-KLN model and  $(\eta/s)_{QGP}=0.16$ . The experimental data are from the STAR, which are measured with the event plane method [19, 20]. This method covers a fraction of contribution from event-by-event flow fluctuations and non-flow contribution mainly including resonance decays and jets. Compared with STAR measurements, the elliptic flow from the VISHNU generally reproduce the data for  $\Lambda$  at 0-10% and 10-40%, and for  $\Xi$  and  $\Omega$  at 0-30% centrality classes. At 40-80%

Au+Au collisions, the model gives rough descriptions of the data for  $\Lambda$  at  $p_T < 1.0$  GeV/c, and for  $\Xi$  and  $\Omega$  at  $p_T < 1.5$  GeV/c, but under-estimates at higher  $p_T$  region. Together with the failed descriptions of elliptic flow for charged hadrons and identified lighter hadrons at 40-80% collisions in Refs. [28, 29], it reflects that the VISHNU, with the MC-KLN initial conditions, fails to describe the 40-80% semi-peripheral collisions. This can be probably interpreted as following. In 40-80% collisions, the collision lifetimes are shorter, which leave less time to generate the elliptic flow in the fluid dynamic QGP stage, and the highly dissipative effects in hadronic stage cannot compensate for this.

In Fig. 4, we show the differential elliptic flow of  $\Lambda$ ,  $\Xi$ , and  $\Omega$  at 10-20%, 30-40%, and 50-60% Pb+Pb collisions, which were first given in Ref. [52]. The presented experimental data are measured by the ALICE Collaboration with the scalar product method [23]. The VISHNU theoretical results are calculated with the inputs as presented in Sec. II. Fig. 4 shows that the VISHNU fairly predicts the elliptic flow data for  $\Lambda$ ,  $\Xi$ , and  $\Omega$  at chosen three centrality classes at  $p_T < 2$  GeV/c within the statistical error bars. At  $p_T > 2$  GeV/c, the descriptions of the elliptic flow for  $\Xi$  at 50-60% and for  $\Omega$  at 30-40% and 50-60% become worse. Together with the worse descriptions of elliptic flow data at high- $p_T$  at the RHIC, as shown in Fig. 3, we consider that the viscous corrections probably become too large at high- $p_T$  region, in which the hydrodynamic description in the VISHNU lost its predictive power.

#### IV. MASS ORDERING OF ELLIPTIC FLOW

It is widely accepted that the characteristic mass ordering of differential elliptic flow among various identified hadrons at low- $p_T$  reflects the interplay between radial and elliptic flow, providing more insights into the properties of the QGP fireball. The radial flow creates a depletion in the particle  $p_T$ -spectrum at low values, which increases with increasing particle mass. This leads to heavier particles having a smaller  $v_2$  compared to lighter ones at a given value of  $p_T$ , giving a mass ordering of the  $p_T$  dependent elliptic flow below 1.5 – 2 GeV/c. Such  $v_2$  mass ordering has been discovered in the experiments at both the RHIC and LHC [19, 23, 56–58], which has also been studied within the framework of hydrodynamics [8, 13, 59–61] and blastwave model [8, 62].

Here we investigate the mass ordering of the elliptic flow among various identified hadrons  $\pi$ ,  $K$ ,  $p$ ,  $\Lambda$ ,  $\Xi$ , and  $\Omega$  in Au+Au collisions and Pb+Pb collisions. For clear presentations, the experimental data and our VISHNU results are plotted in separate panels at 0-80% at the RHIC and 30-40% at the LHC. Together with the calculations of elliptic flow of identified hadrons in [29, 30] and in this paper, we find that the VISHNU generally describes the  $v_2(p_T)$  for different identified hadrons at several centrality classes. However, our theoretical results presented in

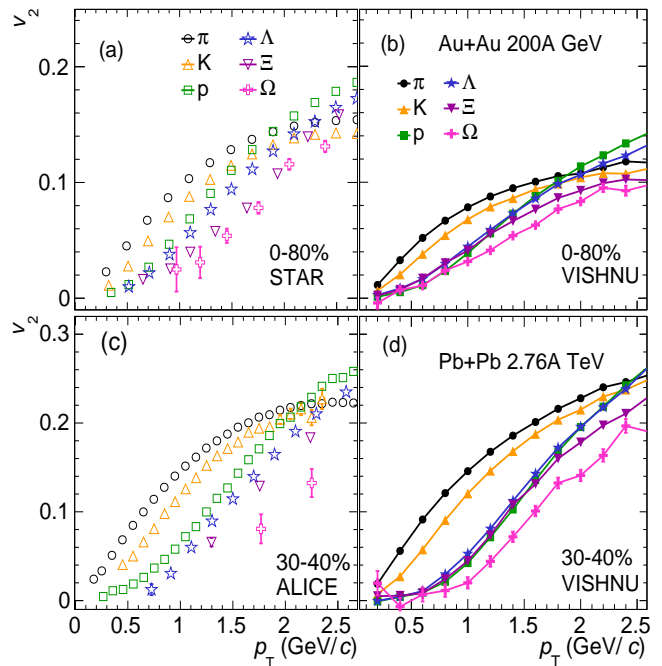


FIG. 5. (Color online) Differential elliptic flow of  $\pi$ ,  $K$ ,  $p$ ,  $\Lambda$ ,  $\Xi$ , and  $\Omega$  at centrality 0-80% in Au+Au collisions at  $\sqrt{s_{NN}}=200$  GeV (top two panels, left: data, right: VISHNU calculations), and at centrality 30-40% in Pb+Pb collisions at  $\sqrt{s_{NN}}=2.76$  TeV (bottom two panels, left: data, right: VISHNU calculations). The measurements of elliptic flow of various hadron species are taken from STAR [15, 20] and ALICE [23].

Fig. 5, compared with the measurements at RHIC and LHC, show that the VISHNU fairly describes the mass ordering among  $\pi$ ,  $K$ ,  $p$ , and  $\Omega$ . But it is hard to see mass ordering among  $p$ ,  $\Lambda$  and  $\Xi$  clearly due to their elliptic flow being almost identical at low  $p_T$  region. This under-prediction for proton leads to an inverse  $v_2$  mass ordering between  $p$  and  $\Lambda$ . Effects of hadronic rescattering on elliptic flow are seen to be particle specific, depending on their scattering cross sections that couple them to the medium [59]. Compared with non-strange hadrons, the multi-strange hadrons are less affected on their differential elliptic flow due to their smaller scattering cross sections. Therefore, re-evaluating the hadronic cross sections in the UrQMD is helpful to improve the description of elliptic flow of various hadron species. Meanwhile, an initial flow could enhance the radial flow in the hadronic stage, which is also expected to improve the description of mass ordering within the framework of the hybrid model.

#### V. SUMMARY AND OUTLOOK

In summary, we studied the  $p_T$ -spectra and elliptic flow of strange and multi-strange hadrons in Au+Au and Pb+Pb collisions within the VISHNU hybrid model. At

both collision systems, we found that, with MC-KLN initial conditions,  $\eta/s = 0.16$  and other inputs, VISHNU generally describes the  $p_T$ -spectra of strange hadron  $\Lambda$  and multi-strange hadrons  $\Xi$  at some centrality classes, but slightly over-estimates for  $\Omega$  at chosen centrality classes. In spite of the normalization issues, the VISHNU well produces the spectra slopes of these three hadrons at chosen centralities. By comparing the elliptic flow of  $\Lambda$ ,  $\Xi$ , and  $\Omega$  in Au+Au collisions and Pb+Pb collisions from VISHNU model with the STAR and ALICE measurements, we found that the VISHNU generally describes the elliptic flow except at 40-80% semi-peripheral collisions. The failed descriptions at 40-80% collisions is probably due to shorter lifetimes of these collisions, which leave less time to generate the elliptic flow in the fluid dynamic QGP stage.

We also compared the mass ordering of  $v_2$  among hadrons  $\pi$ ,  $K$ ,  $p$ ,  $\Lambda$ ,  $\Xi$ , and  $\Omega$  from VISHNU calculations with the STAR and ALICE measurements. The comparisons showed that the elliptic flow mass ordering among various hadron species is not fully described at both RHIC and LHC. The VISHNU fairly describes the mass ordering of  $v_2$  among  $\pi$ ,  $K$ ,  $p$ , and  $\Omega$ , but fails to

reproduce the mass ordering among  $p$ ,  $\Lambda$ , and  $\Xi$  due to slight under-predictions of the elliptic flow of protons. The effects from the initial flow and/or improved UrQMD hadronic cross-sections may solve this issue within the framework of VISHNU, which should be investigated in the near future.

## CONFLICT OF INTERESTS

The author declares that there is no conflict of interests regarding the publication of this paper.

## ACKNOWLEDGMENTS

The author gratefully thanks Huichao Song and Haojie Xu for fruitful discussions and critical reading of the draft. This work was supported in part by the NSFC and the MOST under Grants No. 11435001 and No. 2015CB856900, and the China Postdoctoral Science Foundation under Grant No. 2015M570878. The author especially acknowledges extensive computing resources provided by Tianhe-1A from the National Supercomputing Center in Tianjin, China.

- 
- [1] H. van Hecke, H. Sorge and N. Xu, Phys. Rev. Lett. **81**, 5764 (1998).
- [2] J. Rafelski and B. Muller, Phys. Rev. Lett. **48**, 1066 (1982) [Erratum-ibid. **56**, 2334 (1986)].
- [3] S. Hamieh, K. Redlich and A. Tounsi, Phys. Lett. B **486**, 61 (2000);
- [4] J. Letessier and J. Rafelski, Int. J. Mod. Phys. E **9**, 107 (2000);
- [5] G. Torrieri and J. Rafelski, New J. Phys. **3**, 12 (2001);
- [6] U. W. Heinz, J. Phys. G **25**, 263 (1999).
- [7] G. Torrieri and J. Rafelski, Phys. Lett. B **509**, 239 (2001).
- [8] P. Huovinen, P. F. Kolb, U. W. Heinz, P. V. Ruuskanen and S. A. Voloshin, Phys. Lett. B **503**, 58 (2001).
- [9] V.K. Tiwari, C.P. Singh, Phys. Lett. B **411**, 225 (1997).
- [10] C. Blume and C. Markert, Prog. Part. Nucl. Phys. **66**, 834 (2011).
- [11] N. K. Behera, R. Sahoo and B. K. Nandi, Adv. High Energy Phys. **2013**, 273248 (2013)
- [12] A. Bazavov *et al.*, Phys. Rev. Lett. **113**, no. 7, 072001 (2014).
- [13] X. Zhu and H. Song, Journal of Physics: Conference Series **668**, 012080 (2016).
- [14] J. Adams *et al.* [STAR Collaboration], Phys. Rev. Lett. **92**, 182301 (2004);
- [15] J. Adams *et al.* [STAR Collaboration], Phys. Rev. Lett. **98**, 062301 (2007).
- [16] B. I. Abelev *et al.* [STAR Collaboration], Phys. Rev. C **77**, 044908 (2008).
- [17] M. M. Aggarwal *et al.* [STAR Collaboration], Phys. Rev. C **83**, 024901 (2011);
- [18] J. Adams *et al.* [STAR Collaboration], Phys. Rev. Lett. **95**, 122301 (2005);
- [19] B. I. Abelev *et al.* [STAR Collaboration], Phys. Rev. C **77**, 054901 (2008).
- [20] L. Adamczyk *et al.* [STAR Collaboration], Phys. Rev. Lett. **116**, 062301 (2016).
- [21] B. B. Abelev *et al.* [ALICE Collaboration], Phys. Rev. Lett. **111**, no. 22, 222301 (2013).
- [22] B. B. Abelev *et al.* [ALICE Collaboration], Phys. Lett. B **728**, 216 (2014) [Erratum-ibid. B **734**, 409 (2014)].
- [23] B. B. Abelev *et al.* [ALICE Collaboration], JHEP **1506**, 190 (2015).
- [24] Md. Nasim *et al.* Adv. High Energy Phys. **2015**, 197930 (2015)
- [25] S. Voloshin and Y. Zhang, Z. Phys. C **70**, 665 (1996).
- [26] B. Schenke, S. Jeon and C. Gale, Phys. Lett. B **702**, 59 (2011);
- [27] Z. Qiu, C. Shen and U. Heinz, Phys. Lett. B **707**, 151 (2012).
- [28] H. Song, S. A. Bass, U. Heinz, T. Hirano and C. Shen, Phys. Rev. C **83**, 054910 (2011) Erratum: [Phys. Rev. C **86**, 059903 (2012)].
- [29] H. Song, S. A. Bass and U. Heinz, Phys. Rev. C **83**, 054912 (2011) [Erratum-ibid. C **87**, 019902 (2013)].
- [30] H. Song, S. Bass and U. W. Heinz, Phys. Rev. C **89**, no. 3, 034919 (2014).
- [31] H. Song, Nucl. Phys. A **904-905**, 114c (2013);
- [32] H. Petersen, J. Steinheimer, G. Burau and M. Bleicher, Eur. Phys. J. C **62**, 31 (2009).
- [33] T. Hirano, U. W. Heinz, D. Kharzeev, R. Lacey and Y. Nara, Phys. Lett. B **636**, 299 (2006).
- [34] D. Teaney, J. Lauret and E. V. Shuryak, Phys. Rev. Lett. **86**, 4783 (2001).
- [35] P. Bozek, Phys. Lett. B **699**, 283 (2011).

- [36] S. Takeuchi, K. Murase, T. Hirano, P. Huovinen and Y. Nara, Phys. Rev. C **92**, no. 4, 044907 (2015)
- [37] H. Song, S. A. Bass and U. Heinz, Phys. Rev. C **83**, 024912 (2011);
- [38] H. Song and U. Heinz, Phys. Lett. **B658**, 279 (2008);
- [39] H. Song and U. Heinz, Phys. Rev. C **77**, 064901 (2008);
- [40] S. A. Bass *et al.*, Prog. Part. Nucl. Phys. **41**, 255 (1998).
- [41] M. Bleicher *et al.*, J. Phys. G **25**, 1859 (1999).
- [42] Y. Aoki, Z. Fodor, S. D. Katz and K. K. Szabo, Phys. Lett. B **643**, 46 (2006);
- [43] Y. Aoki *et al.*, JHEP **0906**, 088 (2009).
- [44] S. Borsanyi *et al.* (Wuppertal-Budapest Collaboration), JHEP **1009**, 073 (2010);
- [45] A. Bazavov *et al.*, Phys. Rev. D **85**, 054503 (2012).
- [46] P. Huovinen and P. Petreczky, Nucl. Phys. **A837**, 26 (2010).
- [47] C. Shen, U. Heinz, P. Huovinen and H. Song, Phys. Rev. C **82**, 054904 (2010).
- [48] H. J. Drescher, A. Dumitru, A. Hayashigaki and Y. Nara, Phys. Rev. C **74**, 044905 (2006).
- [49] H. J. Drescher and Y. Nara, Phys. Rev. C **75**, 034905 (2007)
- [50] H. J. Drescher and Y. Nara, Phys. Rev. C **76**, 041903(R) (2007).
- [51] H. Song, S. A. Bass, U. Heinz, T. Hirano and C. Shen, Phys. Rev. Lett. **106**, 192301 (2011) [Erratum-ibid. **109**, 139904 (2012)];
- [52] X. Zhu, F. Meng, H. Song and Y. X. Liu, Phys. Rev. C **91**, no. 3, 034904 (2015).
- [53] C. Shen, Z. Qiu, H. Song, J. Bernhard, S. Bass and U. Heinz, Comput. Phys. Commun. **199**, 61 (2016).
- [54] A. Adare *et al.* [PHENIX Collaboration], Phys. Rev. C **93**, no. 2, 024901 (2016).
- [55] K. Aamodt *et al.* [ALICE Collaboration], Phys. Rev. Lett. **106**, 032301 (2011).
- [56] J. Adams *et al.* [STAR Collaboration], Phys. Rev. C **72**, 014904 (2005);
- [57] M. Issah *et al.* [PHENIX Collaboration]. [nucl-ex/0604011](#).
- [58] R. Snellings, [arXiv:1411.7690](#) [nucl-ex].
- [59] T. Hirano, U. W. Heinz, D. Kharzeev, R. Lacey and Y. Nara, Phys. Rev. C **77**, 044909 (2008);
- [60] P. Bozek, AIP Conf. Proc. **1422**, 34 (2012).
- [61] H. Song, F. Meng, X. Xin and Y. X. Liu, J. Phys. Conf. Ser. **509**, 012089 (2014).
- [62] C. Adler *et al.* [STAR Collaboration], Phys. Rev. Lett. **87**, 182301 (2001).